Material Modeling of Reinforced Concrete

Modèle de comportement du béton armé

Modelle für das Stahlbetonverhalten

KURT H. GERSTLE
Professor of Civil Engineering
University of Colorado
Boulder, CO, USA

SUMMARY

This report presents an overview of the current state of knowledge of the behavior of reinforced concrete and its formulation for finite-element analysis. Aspects of material behavior covered include elastic and inelastic response, including yielding of the steel and crushing and cracking of concrete, leading to anisotropic action, force transfer across cracks, and bond deterioration between steel and concrete. The importance of assessing the influence of these different phenomena is pointed out.

RESUME

Ce rapport donne un aperçu de l'état actuel des connaissances sur le comportement du béton armé et sur sa formulation pour l'analyse par la méthode des éléments finis. Les différents aspects du comportement des matériaux comprennent, outre le comportement élastique et inélastique, la plastification de l'acier, la fissuration et l'écrasement du béton; ceci conduit à un effet d'anisotropie, à une transmission d'efforts à travers les fissures et à une diminution de l'adhérence entre acier et béton. Il est important d'estimer correctement les différents phénomènes.

ZUSAMMENFASSUNG

Dieser Bericht gibt einen Überblick über den gegenwärtigen Stand der Kenntnis des Stahlbetons und seiner Formulierung für Berechnungen mit finiten Elementen. Die behandelten Aspekte des Materialverhaltens betreffen elastisches und inelastisches Verhalten einschliesslich Fliessen des Stahls, Rissbildung und Versagen des Betons. Diese Erscheinungen führen zu anisotropem Verhalten, zur Kraftübertragung an Rissen und zur Verschlechterung des Verbunds zwischen Stahl und Beton. Es ist wichtig, die verschiedenen Phänomene richtig einzuschätzen.

1. FINITE-ELEMENT FORMULATION

1.1 General Formulation

Finite-element analysis is based on subdividing the structure into a number of discrete elements, connected to each other at individual joints, as shown in Fig. 1. The nodal displacements $\{\Delta\}$ are determined by the stiffness, or displacement, method, in which the nodal forces $\{X\}$ are related to these displacements by the structure stiffness matrix $[K]$:

$$\{X\} = [K]\{\Delta\} \quad . \tag{1}$$

The matrix $[K]$ contains the material properties; if these can be represented by linear relations, as in elastic analysis, the stiffnesses are constants, and the determination of the unknowns is a straightforward problem of solving a set of linear simultaneous equations. Non-linear material behavior, as in reinforced concrete, is often modelled as piecewise-linear, and solved in a step-by-step fashion.

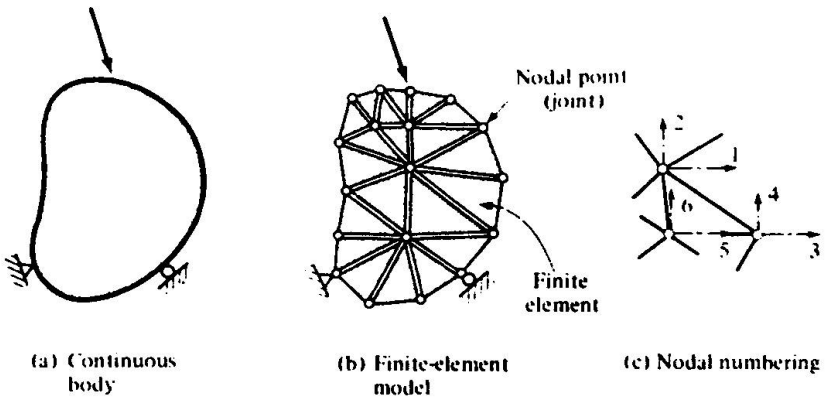

Fig. 1 Finite-element Model

The structure stiffness matrix $[K]$ can be assembled by superposition of the element stiffness matrices $[k]$; equilibrium demands that

$$[K] = \sum_i [k^i] \tag{2}$$

The stiffness matrix $[k^i]$ contains the material properties of Element i, of volume V:

$$[k^i] = \int_V [B]^T [D][B] \cdot dV, \tag{3}$$

in which $[B]$ is a matrix relating element strains $\{\varepsilon\}$ to its nodal displacements $\{\Delta\}$, and $[D]$ is the material stiffness matrix, relating element stresses $\{\sigma\}$ and strains $\{\varepsilon\}$:

$$\{\sigma\} = [D]\{\varepsilon\} \tag{4}$$

The finite-element formulation thus requires the stress-strain relation of all component materials to be expressed in the form of Eq. 4; for an elastic

isotropic material of modulus E and Poisson's ratio ν under plane stress as shown in Fig. 2, for instance, Eq. 4 is represented by the classical Hooke's Law:

$$\begin{Bmatrix} \sigma_{xx} \\ \sigma_{yy} \\ \sigma_{xy} \end{Bmatrix} = \frac{E}{1-\nu^2} \begin{bmatrix} 1 & \nu & 0 \\ \nu & 1 & 0 \\ 0 & 0 & \frac{1-\nu}{2} \end{bmatrix} \begin{Bmatrix} \varepsilon_{xx} \\ \varepsilon_{yy} \\ \varepsilon_{xy} \end{Bmatrix} \tag{5}$$

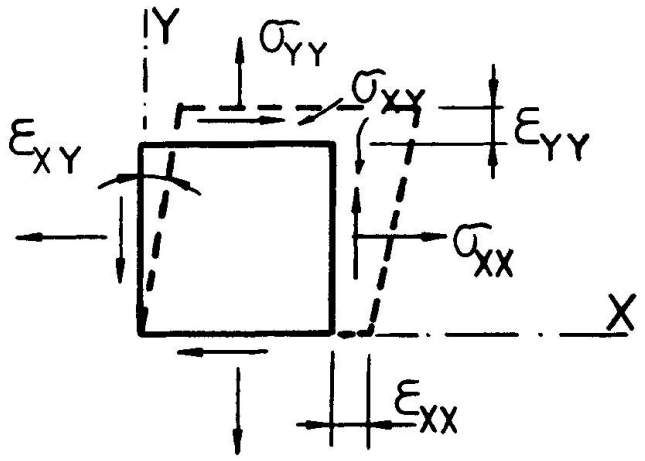

Fig. 2 Plane Element

As at the element level, the stiffnesses of the materials in parallel, as for instance that of concrete, $[D^C]$, and that of steel, $[D^S]$, in the reinforced concrete element shown in Fig. 3, can be superimposed:

$$[D] = [D^C] + [D^S] \quad . \tag{6}$$

The individual stiffnesses must be referred to a common coordinate system; matrix transformations may be required when the principal material directions deviate from each other; if, for instance, the reinforcing layer i along the U axis, of stiffness with respect to this axis

$$[D^i] = p^i E^S \begin{bmatrix} 1 & 0 & 0 \\ 0 & 0 & 0 \\ 0 & 0 & 0 \end{bmatrix}$$

makes an angle α with the reference axes as shown in Fig. 3, then its stiffness matrix $[D^S]$ with respect to the common axes X,Y is given by

$$[D^S] = [\lambda][D^i][\lambda^T] = p^i E^S \begin{bmatrix} \cos^4\alpha & \cos^2\alpha \sin^2\alpha & \cos^3\alpha \sin\alpha \\ \cos^2\alpha \sin^2\alpha & \sin^4\alpha & \cos\alpha \sin^3\alpha \\ \cos^3\alpha \sin\alpha & \cos\alpha \sin^3\alpha & \cos^2\alpha \sin^2\alpha \end{bmatrix} = p^i E^S [T] \tag{7}$$

p^i is the steel ratio A_s/bd, and E^S is the elastic modulus of the steel in the i-th layer; $[\lambda]$ is a matrix of direction cosines given, for instance, in Ref. 1, Eq. 4.15. The problem is now to determine appropriate stiffness matrices $[D^C]$ and $[D^S]$ for the many-faceted behavior of concrete and steel to be inserted into Eq. 6.

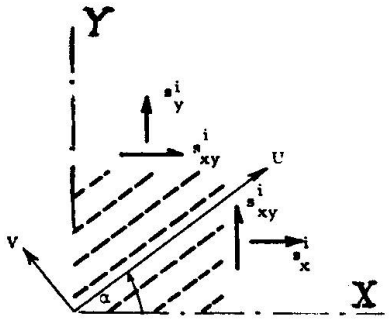

Fig. 3 Reinforcement Stresses

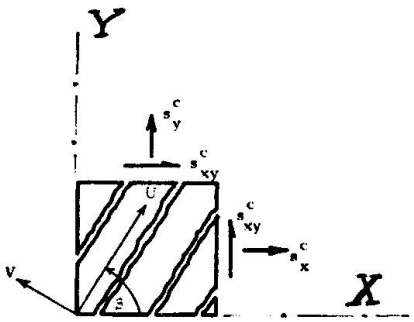

Fig. 4 Concrete Stresses in the Cracked Concrete

1.2 Reinforced Concrete Stiffness

1.2.1 Uncracked Concrete

Before cracking of the concrete, elastic isotropic behavior may be assumed at low stress levels; accordingly, Eq. 5, with E and ν representing the modulus and Poisson's ratio of the plain concrete, is appropriate.

At higher stress levels, non-linear behavior is conveniently expressed by separating the volumetric (hydrostatic, or octahedral normal) response, expressed by the bulk modulus K, and distortional (deviatoric, or octahedral shear) response, expressed by the shear modulus G; the $[D^C]$ matrix for plane stress is given in terms of K and G in Ref. 2 as

$$[D^C] = 4G \frac{3K+G}{3K+4G} \begin{bmatrix} 1 & \frac{3K-2G}{2(3K+G)} & 0 \\ \frac{3K-2G}{2(3K+G)} & 1 & 0 \\ 0 & 0 & \frac{3K+4G}{4(3K+G)} \end{bmatrix} \tag{8}$$

For K and G constant, the elastic relations of Eq. 5 result from Eq. 8; the non-linear behavior of the concrete requires variable tangent or secant moduli K and G; various formulations for these moduli are given in Refs. 3, 4, 5.

Compressive crushing of concrete has been represented using plasticity formulations without and with (6) strain hardening. Isotropic load history effects are formulated in the endochronic theory (7). Directional preference due to prior microcracking as well as post-peak compressive concrete behavior have been formulated (8, 9), and may become important under severe load histories.

1.2.2 Cracked Concrete (10)

Tensile cracking of the concrete will occur in a direction normal to the principal tensile concrete stress when this reaches the tensile cracking strength given, for instance, in Ref. 11. Thereafter a cracked element as shown in Fig. 4 may be visualized, capable of carrying only normal stresses parallel to the cracks:

$$\sigma^c_{uu} = E^c \varepsilon_{uu} \quad \text{or} \quad \begin{Bmatrix} \sigma_{uu} \\ \sigma_{vv} \\ \sigma_{uv} \end{Bmatrix} = E^c \begin{bmatrix} 1 & 0 & 0 \\ 0 & 0 & 0 \\ 0 & 0 & 0 \end{bmatrix} \begin{Bmatrix} \varepsilon_{uu} \\ \varepsilon_{vv} \\ \varepsilon_{uv} \end{Bmatrix} \tag{9}$$

Transformation from the U, V, to the X, Y axes, as discussed earlier in connection with Eq. 7 leads to the cracked concrete stiffness matrix

$$[D^c] = E^c \cdot [T] \; ; \tag{10}$$

the angle α in the [T] matrix should here be replaced by the angle β between the X and the U axes.

Under load histories, cracks in the concrete can successively open and close, as shown, for instance, in Fig. 5. Two sets of cracks at right angles to each other may also occur. These possibilities must be monitored in a step-by-step analysis, and the $[D^c]$ matrix adjusted to reflect the current state of each element.

Non-linear behavior of the cracked concrete can be taken into account by appropriate choice of variable moduli K and G in Eq. 8. Fully plastic response of the cracked concrete can be represented by setting $[D^c] = 0$.

This approach to concrete cracking does not try to predict crack spacing or crack width; the effect of the cracks is "smeared" over the entire element. The predicted crack pattern for a reinforced concrete panel obtained from a formulation as outlined, and shown in Fig. 6a (12) is intended to predict the extent of the cracked zone, and crack directions; the crack spacing is purely a function of the element size selected for analysis: the program indicates one crack through each element. The actual crack pattern observed in test, shown in Fig. 6b, illustrates this difference.

Attempts to predict actual crack spacings and widths have been made by running cracks between elements, rather than smearing them over the elements (13). Because this requires reformulation of the finite-element topology after each crack propagation, this approach does not appear suitable for the analysis of complete concrete structures.

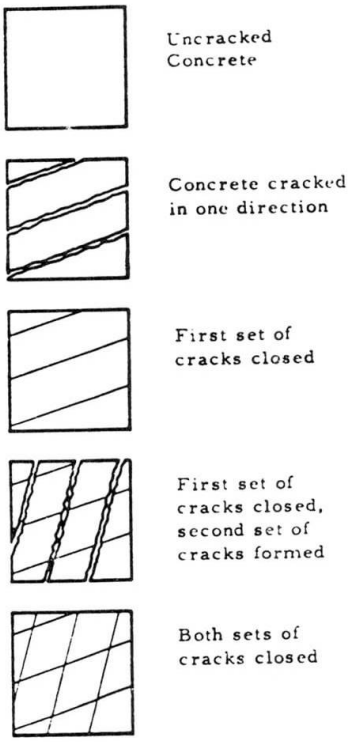

Fig. 5 Crack Modes

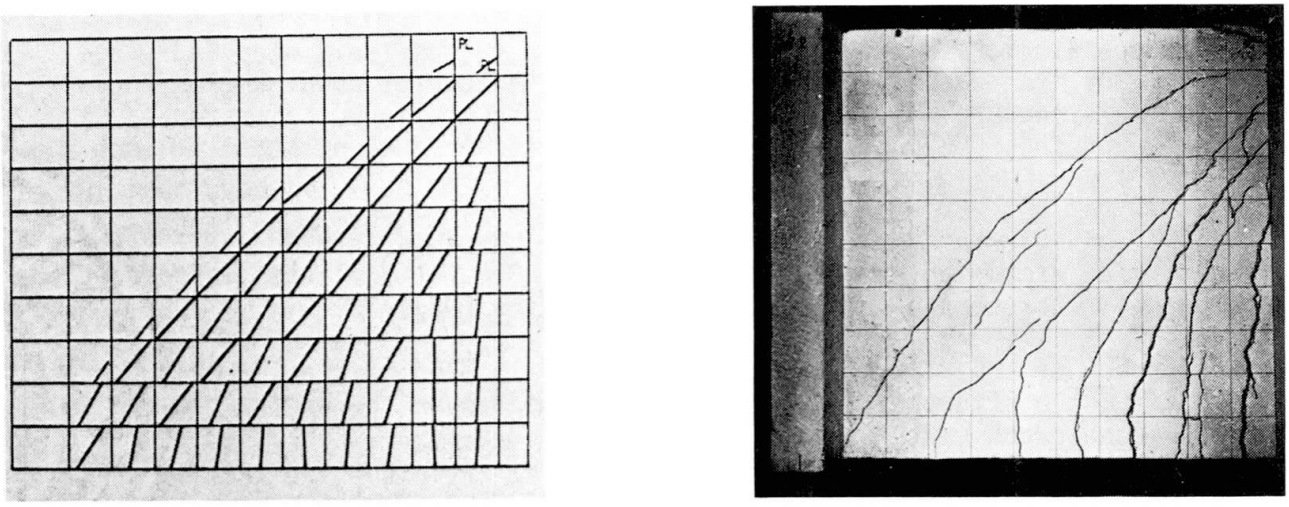

a, Predicted b, Observed

Fig. 6 Crack Pattern

1.2.3 Reinforcement

The case in which the steel in the i-th layer, making an angle α with the reference axes, acts elastically, has already been formulated in Eq. 7; when the plastic limit of this steel is reached, its stiffness vanishes: $[D^i] = 0$. Strain-hardening can also be represented by appropriate modification of Eq. 7. Elastic unloading and reloading of the steel requires monitoring of the steel strains and strain rate, and suitable adjustment of the matrix $[D^i]$.

1.3 Anisotropy of Reinforced Concrete (10)

The reinforcing layer i, represented by Eq. 7, of preferred direction α, as well as cracked concrete of preferred direction β, lead to an anisotropic stiffness matrix [D] when inserted into Eq. 6; this anisotropy will cause deviation of the axes of principal stress and strain within the element: for instance, pure uniaxial tension stress will cause shear distortion of the reinforced concrete, as discussed further below. The degree of anisotropy depends on the reinforcing as well as prior cracking of the concrete.

As an example, we consider the element of previously uncracked concrete and x and y reinforcing of ratios $p_x = 4 \cdot p_y$, as shown in Fig. 7a, inclined at an angle $\alpha = 30^o$ with the principal stress directions (10). Fig. 7b plots the deviation of crack direction, δ, from the principal stress axes, using Eqs. 7 and 6. It is seen that for these conditions, even a small inequality of the principal stresses will cause a great deviation of the cracks from both the principal stress axes, and the directions of reinforcing.

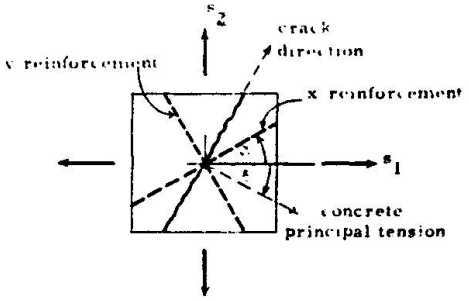

Fig. 7a Deviation of Crack Direction from Total Principal Stress Direction Caused by Reinforcement

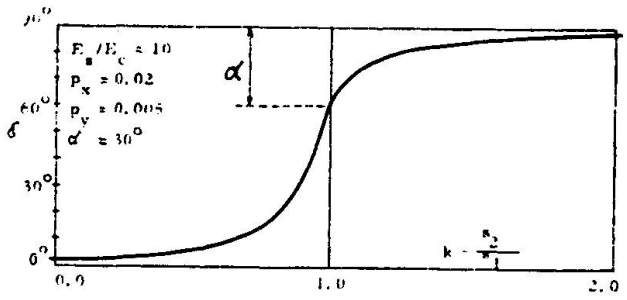

Fig. 7b Effect of Stress State on the Deviation of Concrete Principal Directions

1.4 Experimental Correlation (12)

To check the strains and cracks predicted by Eqs. 4 and 6 experimentally, we refer to the results of a famous test series by Peter (14). Fig. 8 shows the panels tested in uniaxial tension; they contained a grid of equal reinforcing in orthogonal directions, at angles ranging from 0° to 40° with the principal stress direction. Fig. 9 shows the load-extension relations plotted for various values of α; the dashed lines represent predicted response using Eqs. 4 and 6, the solid curves are the measured test results. The actual behavior

beyond cracking shows much greater stiffness than predicted, and none of the discontinuity associated with cracking predicted by theory. This tension-stiffening is due to the bond between steel and concrete between discretely spaced cracks; under increasing load, this bond gradually deteriorates, leading to better agreement between theory and measurement at large extensions.

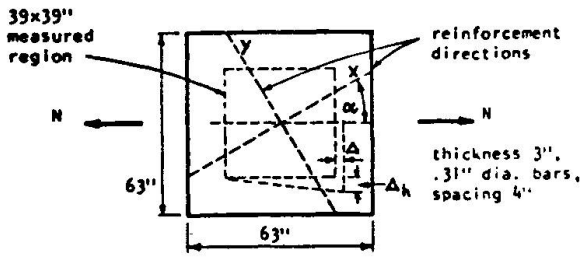

Fig. 8 Peter's Test Panel Subjected to Uniaxial Tension

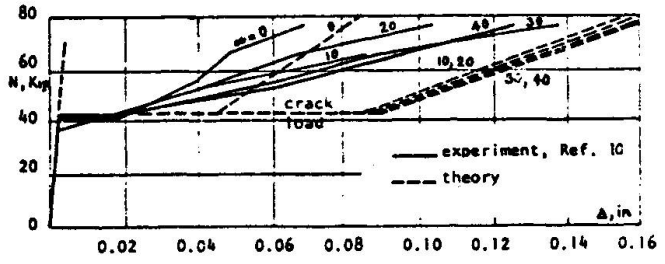

Fig. 9 Load-Extension Relationships

It follows from this observation that a more realistic formulation of the bond-slip behavior between steel and concrete is necessary for prediction of the response of the response of concrete structures with tension cracks. Such formulations will be outlined further on.

The transverse displacement, Δ_h, shown in Fig. 8, is a measure of the shear distortion of the anisotropic panel under uniaxial tension. Fig. 10 shows the predicted, and measured, shear distortion for various reinforcement inclinations α for one load level. For values of less than 30°, the actual shear strain is much less than predicted by the theory which disregards any shear resistance of the crack, as in Eq. 9; in fact, aggregate interlock and dowel action of the bars contribute considerable shear stiffness across cracks, which is indicated by the shaded area of Fig. 10.

It can be concluded that the crack behavior is in fact much more complicated than shown in Figs. 4 or 5, and represented by Eq. 9; these interface shear transfer effects, to be discussed later, should obviously be included in more refined analyses.

2. INTERFACE SHEAR TRANSFER

2.1 Crack Behavior

Fig. 10 shows that the elementary approach which neglects any ability of a concrete crack to transmit stresses can lead to sizable error. In fact, the rough surfaces of narrow cracks can transfer shear stresses through aggregate interlock, which diminishes as the crack becomes wider under further loading.

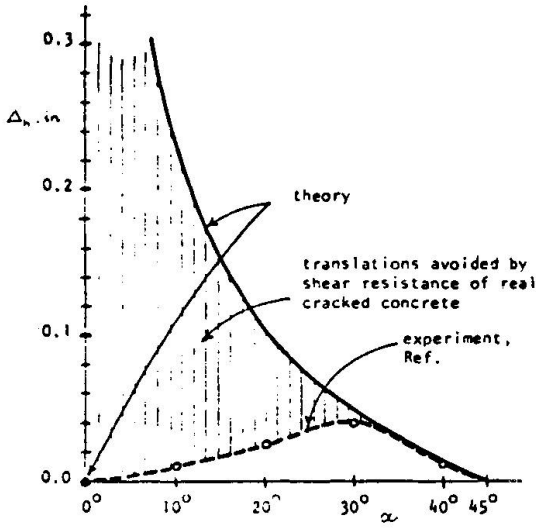

Fig. 10 Effect of Reinforcement Direction on the Transverse Displacement at Load N = 77 Kips

Further, the asperities of the rough crack surfaces will tend to cause a spreading or dilatation of the crack upon sliding, as shown in Fig. 11. When this dilatation is constrained either by surrounding portions of the structure and its supports, or by reinforcing bars crossing the crack, compression results in the concrete which can strengthen the structure but may also under some conditions cause over-stress in the reinforcing steel in tension (15).

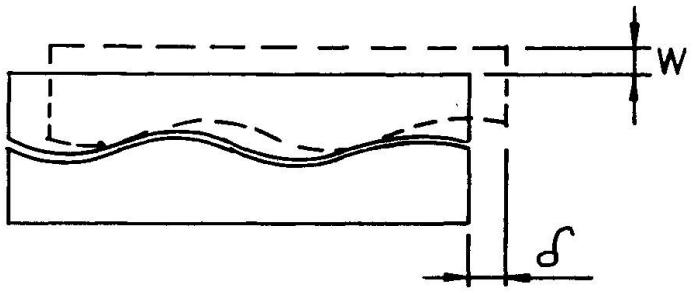

Fig. 11 Crack Displacements

These effects may thus become important under some conditions, particularly under non-proportional load histories in which the principal stress direction changes so that cracks formed initially due to excessive tension become planes of maximum shear under subsequent loads. This has been investigated in the case of nuclear containment vessels which may be under internal pressure followed by earthquake shears (16, 17). It should be realized, however, that these are secondary effects and that many successful analyses, particularly

under proportional loadings, have been performed without considering interface shear transfer.

The detailed behavior of cracks may be considered in two ways: either by looking at each single crack "under a magnifying glass": the shear transfer and dilatation are expressed quantitatively as properties of a joint element which models the crack; this requires knowledge of the location and extent of each crack, something usually not known a priori; further crack propagation requires rearrangement of the element topology from load step to load step. Accordingly, this approach is mainly useful when the safety of a distressed structure, with well-defined existing cracks, is to be determined.

Alternately, when general cracking of a region of the concrete structure may be expected, its shear resistance may be averaged and included as a reduced shear modulus in the material stiffness matrix for the elements representing the cracked region; this approach is clearcut and economical in calculations.

Both of these approaches will be outlined in the following.

2.2 Finite Joint Element

Fig. 12a shows a well-defined crack modelled by a series of joint elements, and Fig. 12b shows one such element in detail; normal and shear stresses, σ and τ, lead to dilatation w and slip δ; these quantities are related by the stiffnesses k_{ij}:

$$\begin{Bmatrix} \sigma \\ \tau \end{Bmatrix} = \begin{bmatrix} k_{11} & k_{21} \\ k_{21} & k_{22} \end{bmatrix} \begin{Bmatrix} w \\ \delta \end{Bmatrix} \tag{11}$$

The element stiffness k_{ij} are, in general, nonlinear functions of stress and displacement levels and rates, as well as prior load histories. Non-zero off-diagonal terms indicate coupling between normal and shear quantities: k_{12} indicates dilatation under slip, which, as previously discussed, can be expected. However, k_{21} indicates sliding under normal stress, which is unlikely. Thus, an unsymmetric stiffness matrix results which will be upsetting not only to the classically-trained analyst, but also to the typical finite-element program.

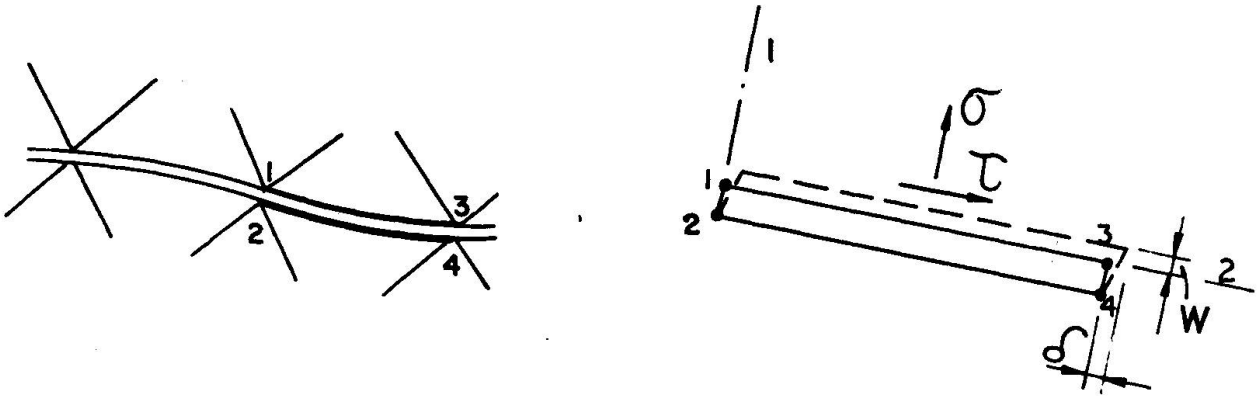

a. Element Grid b. Joint Element

Fig. 12. Joint Element

Little is known about appropriate values for the stiffnesses k_{ij} in Eq. 11. Only the shear, or sliding, stiffness k_{22} has been investigated by a number of researchers (16, 18, 19); in general, shear stress-slip curves appear linear for relatively low stress levels, with diminishing stiffness as cracks get wider; Fig. 13 shows values for the stiffness k_{22} for different crack widths, as obtained in different studies. It might be expected that for higher shear displacements, frictional behavior, analogous to perfect plasticity, might prevail; yet further, the asperities might be sheared off, with consequent loss of shear resistance, as might also prevail under load cycles.

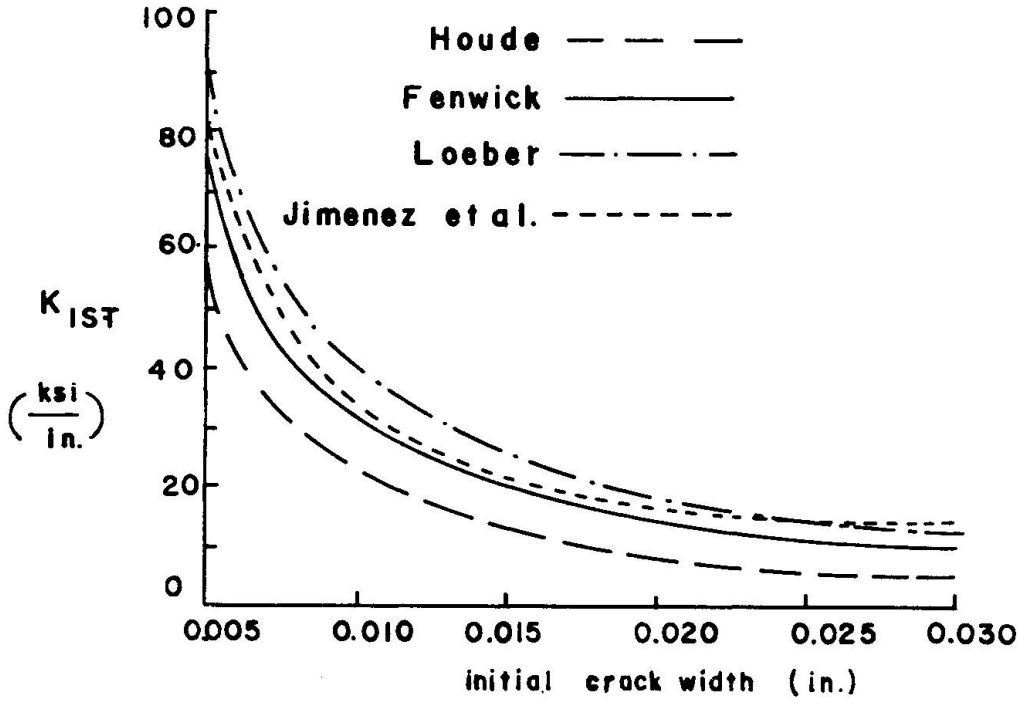

Fig. 13. Crack Shear Stiffness - Crack Width Relation (17)

The normal stress-normal displacement stiffness is strongly sign-dependent: no resistance will be offered to crack opening, while crack closing will have k_{11} = 0 as long as the crack is open, followed by k_{11} proportional to the plain concrete modulus after crack closure. Clearly, any step-by-step program must monitor both current crack widths as well as sense of the displacement.

The coupling term k_{21} is zero, as discussed. No values for k_{12} have been found in the literature, but are badly needed since dilatation during crack slip may contribute importantly to the performance of the cracked structure.

It should be noted that crack displacements are not strains; accordingly, the stiffness k_{ij} have units of F/L^3. The width of the joint element of Fig. 12b may in fact be zero, with opposing joints of identical location. In any case, nodes will have to be so arranged as to allow superposition of the concrete and steel elements for analysis.

2.3 Overall Cracking

In practice, location and nature of any single crack will usually be unknown, and it may become more practical to base the prediction of crack effects on an overall crack pattern as shown in Fig. 14. The degradation of in plane behavior is reflected mainly in the decrease of the shear modulus $G_c = \frac{E}{2(1-\nu)}$ of the plain concrete shown in k_{33} in Eq. 5. This decrease is strongly dependent on crack width and spacing and thus on the degree of reinforcing.

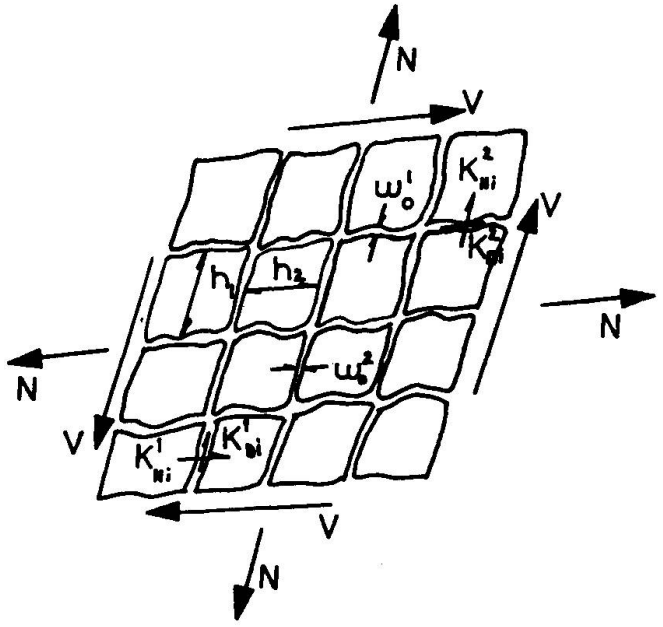

Fig. 14. Generally Cracked Element (17)

The reduced shear modulus G_{cr} or the cracked concrete is given in Ref. 17 as

$$G_{cr} = \left[\frac{1}{h_1\left(\frac{K_N^1}{\beta^1} + K_D^1\right)} + \frac{1}{h_2\left(\frac{K_N^2}{\beta^2} + K_D^2\right)} + \frac{1}{G_c} \right]^{-1} \qquad (12)$$

in which h_1 and h_2 are the expected crack spacings in each crack direction, K_N and K_D are transverse and dowel stiffnesses of the reinforcing, and β represents the effect of aggregate interlock, and is thus a function of the crack width. The three terms in Eq. 12 are nothing more than the effects of the shear displacements due to the cracks in Directions 1, and 2, and those of the uncracked concrete between cracks, respectively.

Figure 15 (20) shows the reduction of shear modulus due to cracking which has been used by different analysts. The range is considerable, from 50 percent to only 10 percent for very wide cracks.

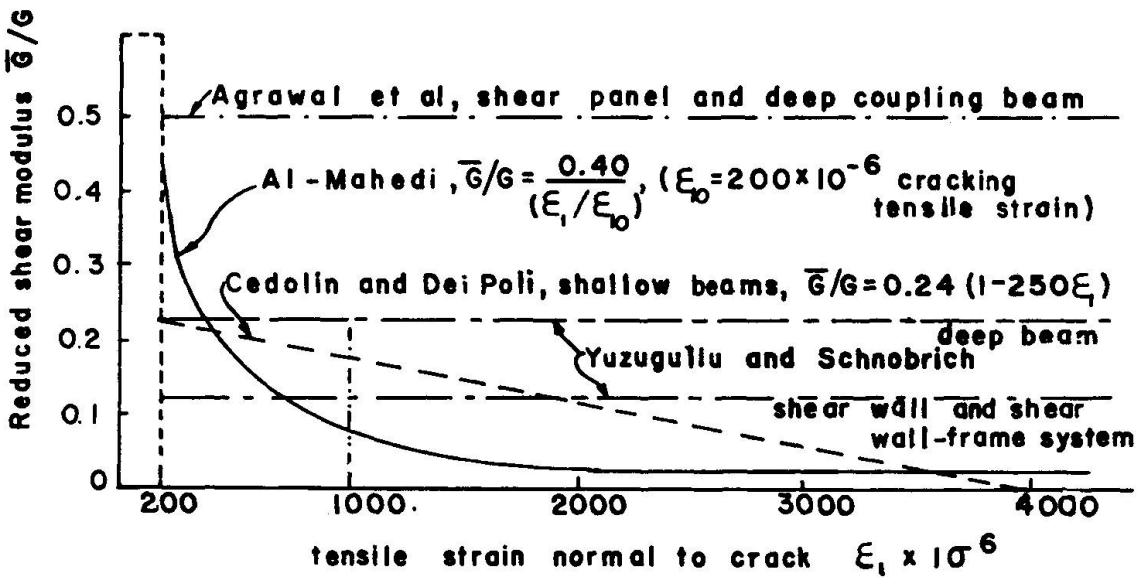

Fig. 15. Shear Stiffness Reduction in Cracked Concrete (20)

Eq. 12 does not consider the important effect of dilatation due to slip of cracks, nor the directional effects of cracking. A more elaborate formulation of the degradation of the concrete due to regularly-spaced cracks which includes both of these effects is presented in Ref. 15. A great deal of laboratory work remains to be done before all experimental parameters necessary for implementation of these formulations are available.

3. BOND SLIP

3.1 General

Fig. 9 showed that the bond between steel and concrete has a considerable effect on the structure behavior after cracking. In fact, if perfect bond without slip is assumed, as in classical reinforced concrete theory, then cracks would not be able to open at all. It follows that rational prediction of crack widths requires knowledge of bond behavior between reinforcing and concrete.

Nevertheless, bond-slip and bond degradation is in many analyses only of secondary importance, and may not affect overall structure behavior significantly, specially for monotonic loading cases.

3.2 Force Transfer and Concrete Cracking

Assuming continuous action along the reinforcing bar, statics of longitudinal forces on a bar element of length dx and perimeter Σ_0 requires that

$$u = \frac{1}{\Sigma_0} \cdot \frac{dP}{dx} \tag{13}$$

that is, the bond stress u is proportional to the rate of change of the axial bar force P. Using this relation, Fig. 16 shows schematically the relation between bond stress, bond slip, crack width, and crack spacing.

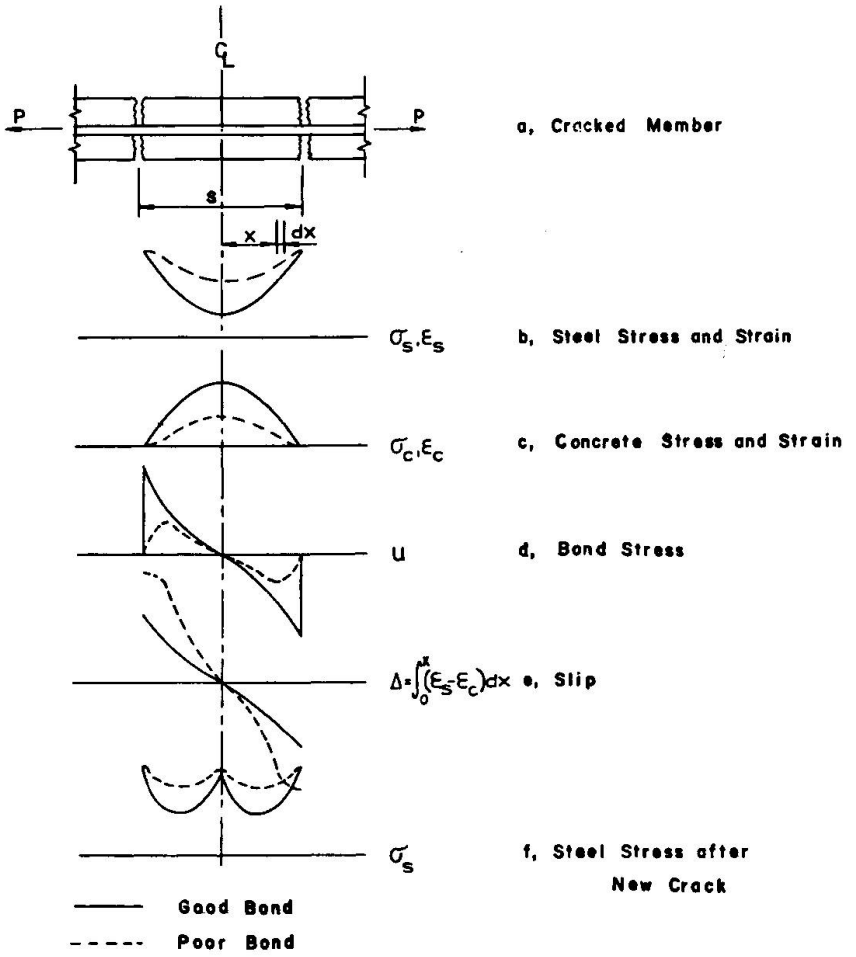

Fig. 16
Relations between Stresses, Bond Slip, and Cracking.

Fig. 16a depicts a portion of a reinforced concrete member between two existing cracks caused by the tension force P in the bar. The steel stress shown in Fig. 16b varies from a maximum at the cracks to a minimum at the uncracked section midway between the cracks. The concrete stress must then pick up the balance of the tension force as shown in Fig. 16c. According to Eq. 13, the bond stress variation must be as shown in Fig. 16d, with a sharp gradient in the vicinity of the cracks.

Under increasing force P, the concrete stresses of Fig. 16c increase until their maximum at the midpoint reaches the tensile strength, at which instance the concrete ruptures, causing a new crack midway between the earlier cracks. From the relations between the bar stresses of Fig. 16b and the bond stresses of Fig. 16d, it follows that the quality of bond strongly affects the occurrence of subsequent cracks. The better the bond, the closer the crack spacing and the narrower the cracks, a well-known fact. After occurrence of the next crack, the steel stress is distributed as in Fig. 16f, and the next cycle of crack formation begins. The nature of this process has been discussed by Broms (21).

Corresponding to the steel and concrete stresses shown in Figs. 16b and 16c, there will be steel and concrete strains ε_s and ε_c; stresses and strains may be proportional for elastic materials, or non-proportional for nonlinear material

behavior. According to this simplified approach, the slip can be found by integrating the difference of steel and concrete strains, starting from the centerline; the crack width should then be equal to the total slip between cracks. In fact, the situation is more complex because a uniaxial analysis as presented here cannot account for the actual three-dimensional strains and crack formation. This real behavior can be represented by a finite-element formulation as outlined in the next section.

3.3 Modeling of Bond Behavior

Bond slip can be modeled by introduction of an appropriate discrete bond-link element, shown in Fig. 17 (13). The spring, of modulus k, represents the resistance offered to slip Δ by the bond stress u:

$$k = \frac{du}{d\Delta} \quad ; \tag{14}$$

the magnitude of this stiffness will be discussed next.

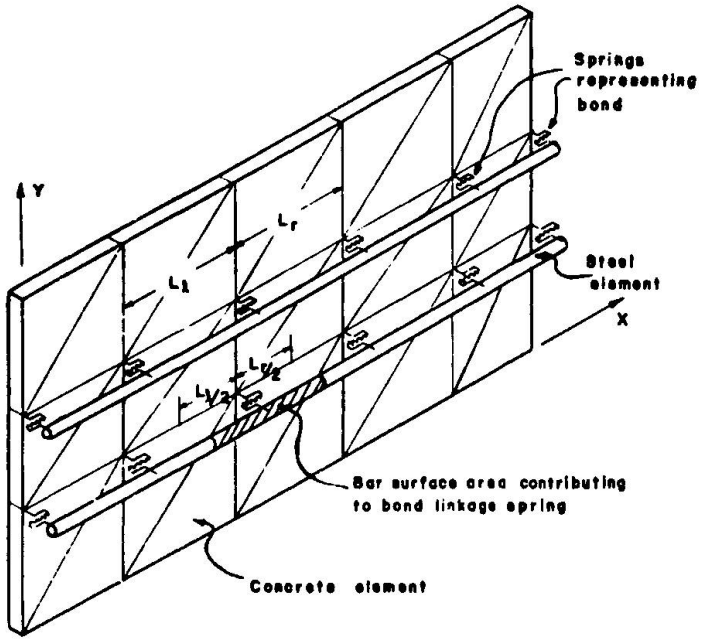

Fig. 17. Bond-Link Element (26)

The splitting effect of the steel bar could be represented by additional degrees of freedom of the link element, but because almost nothing is known about these radial forces, we will not consider them any further.

With sufficient number of these bond-link elements, and knowledge of their stiffness k, the interface behavior between steel and concrete can be modeled.

Experimental determination of the slip resistance k is difficult, and little actual information covering a full range of conditions is available. Fig. 18

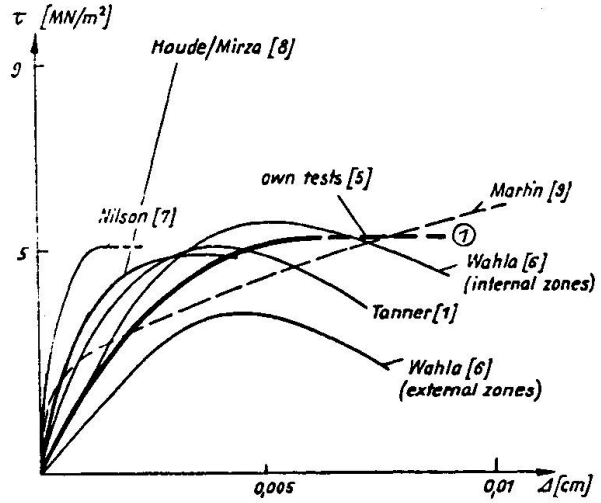

Fig. 18. Bond Stress-Slip Relations (22)

(22) shows the staggering variation of results obtained by different investigators.

Among the more comprehensive tests (covering, however, only one bar size and concrete type) are those of Nilson (23), performed on a specimen as in Fig. 16a, which represents the situation between two existing cracks. The resulting bond stress-slip curves of Fig. 19, which are highly non-linear, indicate that the stiffness k, obtained as the slope of these curves, depends on the distance from the crack faces; it is thus not a unique property of the element, but depends on its neighborhood. This is quite at variance with the basic concepts of finite-element analysis.

Bond-slip under load cycles or load reversals as under seismic shocks can lead to severe bond degradation (24). Morita and Kaku (25) have obtained bond stress-slip relations under cycles of load reversal: Fig. 20a shows one of their typical load cycles which reveals ranges of bearing of the bar ribs against the concrete, as well as frictional resistance. Shipman (26) idealized this behavior for purposes of finite-element analysis as shown in Fig. 20b. Good results were obtained with this model.

Our understanding of these phenomena is just in its infancy.

3.4 Tension Stiffening

Just as in the case of crack behavior, bond can be modeled either by "looking through the magnifying glass", as we have just done, or by taking an averaging approach. The latter has been taken by introducing the concept of tension-stiffening (27). The variable tensile resistance of the concrete surrounding the bar, shown in Fig. 16c, ranging from nil at the crack to full effectiveness at the midpoint between cracks, is averaged by assigning a post-peak range to the tensile concrete stress-strain relation, as shown in Fig. 21. The effectiveness of this concept has been demonstrated in several analyses (28), and has also been extended to the multiaxial case (29).

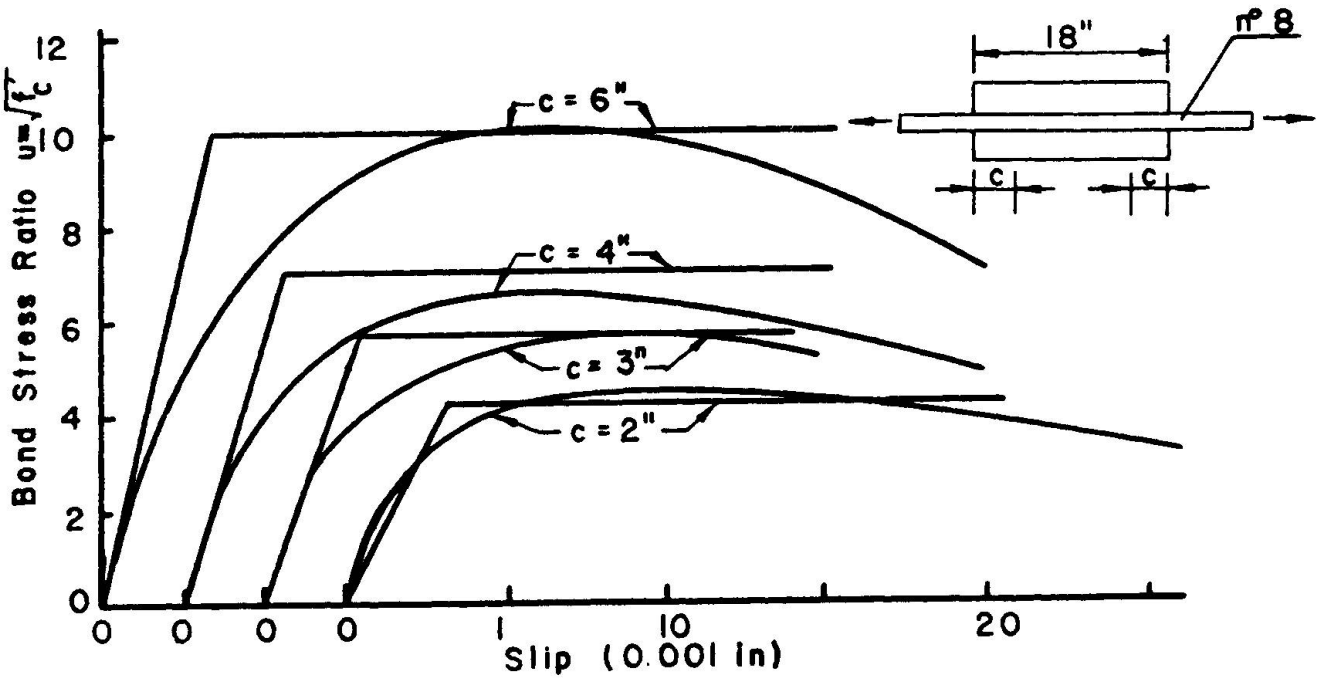

Fig. 19. Bond Stress-Slip Relations of Nilson (23)

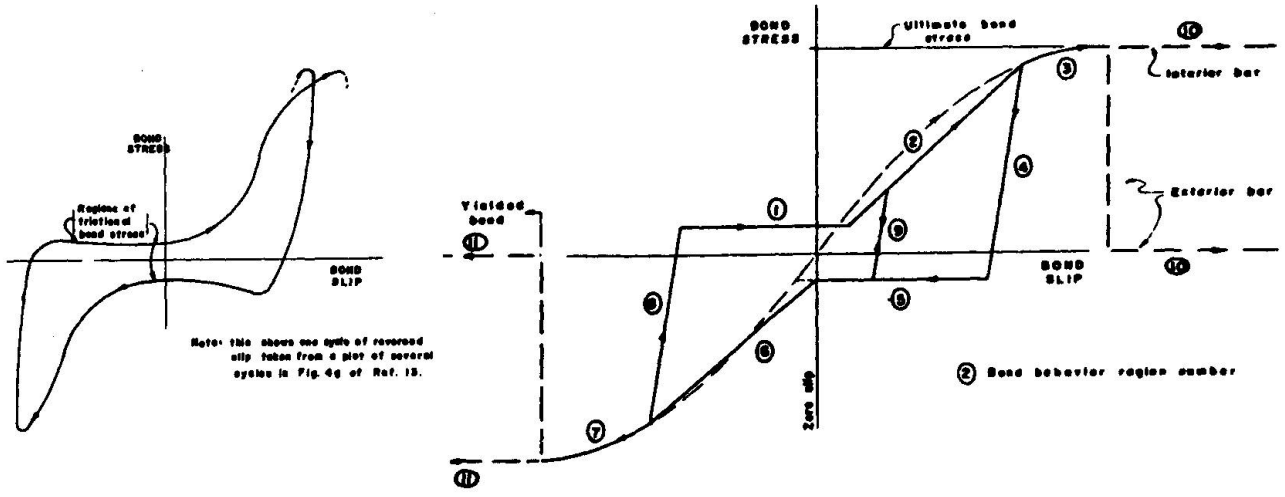

a, Actual Behavior b, Idealization

Fig. 20. Bond Stress-Slip Relations under Load Cycles

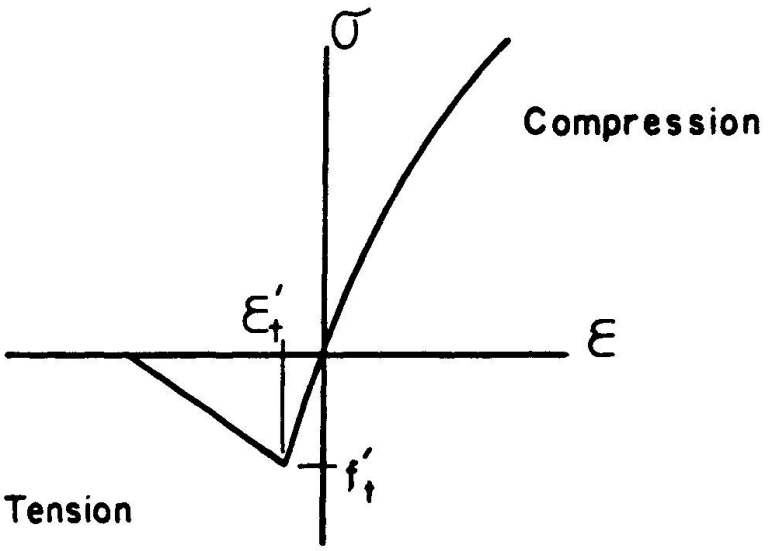

Fig. 21. Concrete Behavior for Tension-Stiffening

4. MODELING PROBLEMS OF CONCRETE STRUCTURES

4.1 Some Unknown Factors

Lastly, we wish to cast a critical eye on the feasibility of realistic modeling of the behavior of reinforced concrete structures.

Only some of the many factors which influence the structural performance have been considered in the foregoing, and most of these have been of non-linear character. The current state of the computer art is such that any non-linear analysis must be considered of developmental nature, and therefore beyond the realm of professional engineering practice. A level head must be preserved regarding the feasibility of realistic analyses under the constraints of office practice.

Looking beyond the basics which have been covered, we wish to draw attention to just a few of the many additional factors which may affect the performance of concrete structures as significantly as those discussed:

1. Time-dependent Behavior of Concrete: Concrete creeps and is likely to affect deformations and cracking.

2. Temperature Effects: Not only seasonal or daily temperature variations, but specially those occurring due to curing of the weak concrete during construction, are quite likely to cause high stresses and cracking.

3. Load Histories: The sequence of load application on real structures during their construction and useful life is quite different from the monotonic loading to failure usually applied in the laboratory. We know very little about the response of plain concrete and its crack- and steel interfaces under general load histories.

Obviously, much remains to be done before we can claim the power to make valid predictions of the response of real structures to real lifetime conditions.

4.2 Case Study

The reinforced concrete panels mentioned earlier (12) showed excellent correlation between predicted and observed behavior under monotonically increasing loads to failure, as shown, for instance, in Fig. 6. However, when subjected to load cycles, any inflated expectations were quickly punctured: as shown in Fig. 22, no correlation at all seemed to exist between analysis and experiment in such cases; actual deformations were larger than predicted by an order of magnitude.

In searching for reasons for these discrepancies, the following simplifications in the analysis were considered:

1. Bond slip had been neglected.
2. Degradation of plain concrete under high stress cycles had been neglected.
3. Simultaneous crack opening in two directions had been neglected.
4. Effect of debris entering open crack upon crack closing had been neglected.
5. Creep of concrete had been neglected.

Of these five cited factors, comparative analyses were performed including No. 1 (26) and No. 2 (9). Fig. 23 summarizes the findings for the very restricted case of one half load cycle: about one third of the discrepancy between calculated and observed behavior can be ascribed to neglect of bond deterioration, the remainder to degradation of the plain concrete. The effect of the other approximations has not been studied.

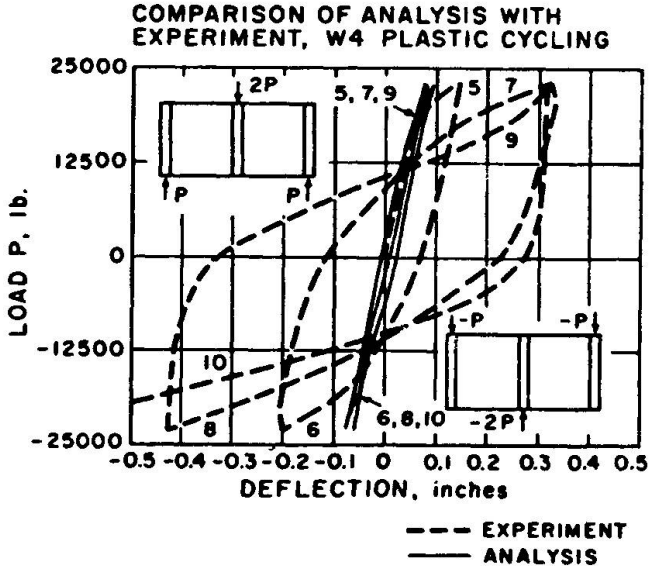

Fig. 22 Predicted and Actual Load-Deflection Curves for Reinforced Concrete Panel under Load Cycles (12)

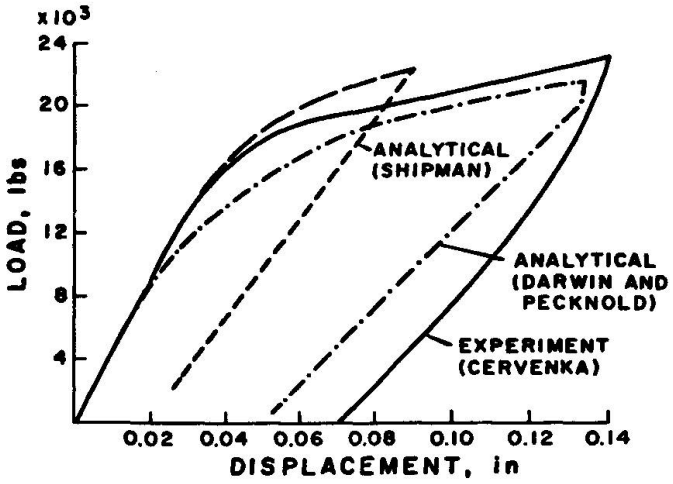

Fig. 23 Results of Two Analyses Compared with Experiment (26)

4.3 Conclusions

Reinforced concrete structures under realistic loading and use conditions are subjected to a great number of complex influences, only a few of which have

been studied in detail, The inclusion of most of these factors appears quite impossible in any routine analysis of real structures.

We do not at this time have much idea of the relative importance of these different effects under specified conditions of use. A systematic investigation of different influences, with the aim of establishing a list of priorities for specific cases, appears useful to achieve the required compromise between reality and simplicity which underlies the engineering approach.

ACKNOWLEDGEMENTS

The major portion of this report was written while the author was Senior Fellow of the Alexander von Humboldt-Foundation, Bonn, Germany, and on sabbatical leave from the University of Colorado, Boulder. Thanks are due for this financial support, as well as to the Technical University of Darmstadt, Germany, and to Professor Gerhart Mehlhorn, for their hospitality.

REFERENCES

1. Zienkiewicz, O.C., "The Finite Element Method in Engineering Science," 2nd Ed., McGraw-Hill, London, 1971.

2. Kupfer, H.B., and K.H. Gerstle, "Behavior of Concrete under Biaxial Stresses," Proc. A.S.C.E., Jul. E.M.D., Vol. 99, No. EM4, August 1973.

3. Cedolin, L., Y.R.J. Crutzen, S. Dei Poli, "Stress-Strain Relationship and Ultimate Strength of Concrete under Triaxial Loading Conditions," Proc. A.S.C.E., Jul. E.M.D., Vol. 103, No. EM3, June 1977.

4. Kotsovos, M.D., and J.B. Newman, "Generalized Stress-Strain Relations for Concrete," Proc. A.S.C.E., Jul. E.M.D., Vol. 104, No. EM4, August 1978.

5. Gerstle, K.H., H. Aschl, et al., "Behavior of Concrete under Multiaxial Stress States," Proc. A.S.C.E., Jul. E.M.D., 1980.

6. Chen, W.F., "Constitutive Equations for Concrete," Rept. I.A.B.S.E., Vol. 28, Colloquium Kopenhagen, 1979.

7. Bazant, Z.P., and P.D. Bhat, "Endochronic Theory of Inelasticity and Failure of Concrete," Proc. A.S.C.E., Jul. E.M.D., Vol. 102, No. EM4, August 1979.

8. Liu, T.C.Y., A.H. Nilson, F.O. Slate, "Biaxial Stress-Strain Relations for Concrete," Proc. A.S.C.E., Jul. Struct. Div., Vol. 98, No. ST5, May 1972.

9. Darwin, D., and D.A. Pecknold, "Analysis of R.C. Shear Panels under Cyclic Loading," Proc. A.S.C.E., Jul. Struct. Div., Vol. 102, No. ST2, February 1976.

10. Cervenka, V., and K.H. Gerstle, "Inelastic Analysis of Reinforced Concrete Panels: Theory," Pubs. I.A.B.S.E., Vol. 31-II, 1971.

11. Kupfer, H.B., H.K. Hilsdorf, H. Ruesch, "Behavior of Concrete under Biaxial Stress," Jul. A.C.I., Vol. 66, No. 8, August 1969.

12. Cervenka, V., and K.H. Gerstle, "Inelastic Analysis of Reinforced Concrete Panels: Experimental Verification and Application," Pubs. I.A.B.S.E., Vol. 32-II, 1972.

13. Ngo, D., and A.C. Scordelis, "Finite Element Analysis of Reinforced Concrete Beams," Jul. A.C.E., Vol. 64, No. 3, March 1967.

14. Peter, J., "Zur Bewehrung von Scheiben und Schalen ...," Dr.-Ing. Dissertation, T.H. Stuttgart, 1964.

15. Bazant, Z.P., and T. Tsubaki, "Friction-Dilatancy Model for Cracked Reinforced Concrete," Struct. Engin. Report No. 79-8/640f, Dept. of Civil Engin., Northwestern Univ., Evanston, Ill., August 1979.

16. Jimenez, R., P. Gergely, R.N. White, "Shear Transfer across Cracks in Reinforeced Concrete," Report No. 78-4, Department of Structural Engineering, Cornell Univ., Ithaca, N.Y., August 1979.

17. Buyukozturk, O., J.J. Connor, P. Leombonni, "Research on Modeling Shear Transfer in Reinforced Concrete Nuclear Structures," Proc. S.M.I.R.T., Berlin, Germany, August 1979.

18. Walraven, J.C., E. Vos, H.W. Reinhardt, "Experiments on Shear Transfer in Cracked Concrete," Proc. I.A.S.S. Symposium, Darmstadt, Germany, July 1978.

19. Fenwick, R.C., and T.O. Pauley, "Mechànism of Shear Resistance in Concrete Beams," Proc. A.S.C.E., Jul. Struct. Div., Vol. 94, No. ST10, Oct. 1968.

20. Al-Mahaidi, R.S.H., "Nonlinear Finite Element Analysis of Reinforced Concrete Deep Members," Report No. 79-1, Dept. of Struct. Engin., Cornell University, January 1979.

21. Broms, B.B., "Technique for Investigation of Internal Cracks in Reinforced Concrete Members," Jul. A.C.I., Vol. 62, January 1965.

22. Dörr, K., "Bond Behavior of Ribbed Reinforcement under Transversal Pressure," Proc. I.A.S.S. Symp. Darmstadt, Germany, July 1978.

23. Nilson, A.H., "Bond Stress-Slip Relation in Reinforced Concrete," Struct. Eng. Dept. No. 345, Cornell University, December 1971.

24. Bresler, B., and V. Bertero, "Behavior of Reinforced Concrete under Repeated Loads," Proc. A.S.C.E., Jul. Struct. Div., Vol. 94, No. ST6, June 1968.

25. Morita, S., and T. Kaku, "Local Bond Stress-Slip Relationship under Repeated Loading," Proc. I.A.B.S.E. Symp., Lisbon, Portugal, Sept. 1973.

26. Shipman, J.M., and K.H. Gerstle, "Bond Deterioration in Concrete Panels under Load Cycles," Jul. A.C.E., Vol. 76, No. 2, February 1979.

27. Scanlon, A. and D.W. Murray, "Time-Dependent Deflections of Reinforced Concrete Slabs," Proc. A.S.C.E., Jul. Struct. Div., Vol. 100, No. ST9, Sept. 1974.

28. Gilbert. R.I., and R.F. Warner, "Tension-Stiffening in Reinforced Concrete Slabs." Proc. A.S.C.E., Jul. Struct. Div., Vol. 104, No. ST12, December 1978.

29. Geistefeld, H., "Multiaxial Tension-Stiffening Constitutive Relations for Concrete," Proc. I.A.S.S. Symposium, Darmstadt, Germany, July 1978.

Leere Seite
Blank page
Page vide